NASA TN D-465

TECHNICAL NOTE

D-465

THE MAGNETIC FIELD OF A FINITE SOLENOID

By Edmund E. Callaghan and Stephen H. Maslen

Lewis Research Center
Cleveland, Ohio

NATIONAL AERONAUTICS AND SPACE ADMINISTRATION

WASHINGTON October 1960

NATIONAL AERONAUTICS AND SPACE ADMINISTRATION

TECHNICAL NOTE D-465

THE MAGNETIC FIELD OF A FINITE SOLENOID

By Edmund E. Callaghan and Stephen H. Maslen

E-900

SUMMARY

The axial and radial fields at any point inside or outside a finite solenoid with infinitely thin walls are derived. Solution of the equations has been obtained in terms of tabulated complete elliptic integrals. For the axial field an accurate approximation is given in terms of elementary functions. Fields internal and external to the solenoid are presented in graphical form for a wide variety of solenoid lengths.

CQ-1

INTRODUCTION

The recent great interest in plasmas either as a source of energy or as a propulsion device has resulted in a greatly renewed interest in the magnetic fields produced by various configurations of electromagnets. Of the possible methods of plasma confinement by far the most promising appears to be the use of magnetic fields (ref. 1).

The calculation of the fields generated by various electromagnetic configurations such as loops, finite helical solenoids, and infinite solenoids has been treated by the early classical physicists, but only the simplest cases such as the single loop have been calculated for the entire field both inside and outside the loop (e.g., ref. 2). In other cases such as the helical solenoid or the finite solenoid the calculations have been limited to the axis (ref. 3). Derivations of the off-axis positions have been done by Foelsch (ref. 4), and the solutions are obtainable by means of a large number of approximate expressions which are valid over restricted ranges of size or position. The principal difficulty in the calculation of the fields of nearly all configurations has resulted from the fact that the integral solution cannot be achieved without the use of various elliptic integrals. Even though many of these are tabulated, the calculations involved are laborious. Such calculations can, however, be made using modern high-speed computers since machine programs have or can be written for many of the elliptic functions.

The purpose of this report is twofold: (1) to derive the equations of the axial and radial field at any point within or outside a finite solenoid in terms of standard tabulated functions and (2) to plot these fields for a number of solenoids.

SYMBOLS

A_θ	magnetic vector potential component in θ-direction
a	coil radius
B_r, B_z	radial and axial magnetic induction component
E	complete elliptic integral, second kind
i	current in each filament
K	complete elliptic integral, first kind
k	$\sqrt{4ar/[\xi^2 + (a + r)^2]}$
L	coil length
n	number of turns per unit coil length
r, θ, z	cylindrical coordinates
λ_o	Heuman lambda function
μ	permeability
$\xi_\pm$	$z \pm \frac{L}{2}$
φ	$\tan^{-1}\left\lvert\frac{\xi}{a - r}\right\rvert$

DERIVATION OF EQUATIONS

Consider a solenoid as shown in the following sketch:

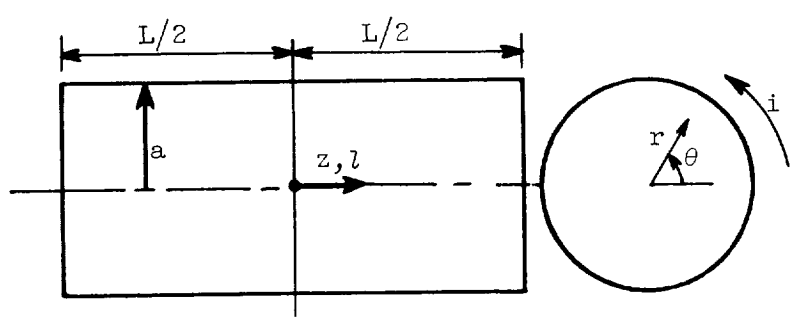

The magnetic field due to this coil is given in terms of the vector potential $\vec{A}$ by

$$\vec{B} = \nabla \times \vec{A} \tag{1}$$

where, for the geometry assumed, only the A_θ component can be nonzero. Then equation (1) yields simply

$$\left.\begin{aligned} B_r &= -\frac{\partial A_\theta}{\partial z} \\ B_z &= \frac{1}{r}\frac{\partial (rA_\theta)}{\partial r} \end{aligned}\right\} \tag{2}$$

For a single circular filament, one has

$$A_\theta = \frac{\mu i}{4\pi}\oint \frac{a \cos\theta \, d\theta}{R}$$

where R is the distance from the local point on the filament to the field point. For a solenoid made up of a series of n filaments per unit length, we have then

$$A_\theta = \frac{a\mu n i}{2\pi}\int_{-L/2}^{L/2} dl \int_0^\pi \frac{\cos\theta \, d\theta}{\sqrt{(z-l)^2 + r^2 + a^2 - 2ar\cos\theta}}$$

or

$$A_\theta = \frac{a\mu n i}{2\pi}\int_{\xi_-}^{\xi_+} d\xi \int_0^\pi \frac{\cos\theta \, d\theta}{\sqrt{\xi^2 + r^2 + a^2 - 2ar\cos\theta}} \tag{3}$$

where $\xi = z - l$, $\xi_\pm = z \pm L/2$, and l is the axial distance from the origin to the filament. On integrating with respect to ξ, this becomes

$$A_\theta = \frac{a\mu n i}{2\pi}\int_0^\pi \cos\theta \ln\left[\xi + \sqrt{\xi^2 + r^2 + a^2 - 2ar\cos\theta}\right]_{\xi_-}^{\xi_+} d\theta \tag{4}$$

A more convenient form can be found by integrating by parts:

$$A_\theta = \frac{a\mu n i}{2\pi}\left[\sin\theta \ln\left[\xi + \sqrt{\xi^2 + r^2 + a^2 - 2ar\cos\theta}\right]_{\xi_-}^{\xi_+}\right]_{\theta=0}^{\theta=\pi}$$

$$- \frac{a\mu n i}{2\pi}\int_0^\pi \left[\frac{ar\sin^2\theta \, d\theta}{\left(\xi + \sqrt{\xi^2 + r^2 + a^2 - 2ar\cos\theta}\right)\sqrt{\xi^2 + r^2 + a^2 - 2ar\cos\theta}}\right]_{\xi_-}^{\xi_+}$$

The first term vanishes. On multiplying the integrand by $\frac{\sqrt{\xi^2 + r^2 + a^2 - 2ar \cos \theta} - \xi}{\sqrt{\xi^2 + r^2 + a^2 - 2ar \cos \theta} - \xi}$, rearranging terms, and observing that use of the limits eliminates one term, there follows

$$A_\theta = \frac{a^2 \mu n i r}{2\pi} \int_0^\pi \left[\frac{\xi \sin^2\theta \, d\theta}{(a^2 + r^2 - 2ar \cos \theta)\sqrt{\xi^2 + r^2 + a^2 - 2ar \cos \theta}} \right]_{\xi_-}^{\xi_+} \tag{5}$$

The two magnetic-field components can now be easily obtained. The radial field is found by differentiating equation (3) and yields

$$B_r = - \frac{\partial A_\theta}{\partial z} = - \frac{a \mu n i}{2\pi} \int_0^\pi \left[\frac{\cos \theta \, d\theta}{\sqrt{\xi^2 + r^2 + a^2 - 2ar \cos \theta}} \right]_{\xi_-}^{\xi_+} \tag{6}$$

To get B_z, first evaluate $\partial A_\theta / \partial r$ from equation (4). The result, proceeding as in the case of obtaining equation (5), is

$$\frac{\partial A_\theta}{\partial r} = - \frac{a \mu n i}{2\pi} \int_0^\pi \left[\frac{\xi \cos \theta (r - a \cos \theta) d\theta}{(r^2 + a^2 - 2ar \cos \theta)\sqrt{\xi^2 + r^2 + a^2 - 2ar \cos \theta}} \right]_{\xi_-}^{\xi_+} \tag{7}$$

If equations (5) and (7) are put into (2), the result is

$$B_z = \frac{1}{r} \frac{\partial (r A_\theta)}{\partial r} = \frac{a \mu n i}{2\pi} \int_0^\pi \left[\frac{\xi (a - r \cos \theta) d\theta}{(r^2 + a^2 - 2ar \cos \theta)\sqrt{\xi^2 + r^2 + a^2 - 2ar \cos \theta}} \right]_{\xi_-}^{\xi_+} \tag{8}$$

Equations (6) and (8) describe the magnetic field due to a finite solenoid. Numerical results can readily be found by integrating these equations on a computer. However, the results can also be expressed in terms of standard elliptic integrals, which are already tabulated. This we proceed to do.

Consider B_r. This can be evaluated by use of formulas 291.03 and 412.01 (noting the special case of $\alpha^2 = k^2$) of reference 5. One has successively,

$$B_r = - \frac{a \mu n i}{\pi} \left[\frac{1}{\sqrt{\xi^2 + (r + a)^2}} \int_0^{K(k)} \frac{1 - (2 - k^2) sn^2 u \, du}{1 - k^2 sn^2 u} \right]_{\xi_-}^{\xi_+}$$

$$B_r = -\frac{a\mu ni}{\pi}\left[\frac{1}{k^2\sqrt{\xi^2 + (r + a)^2}}\int_0^{K(k)}\left(2 - k^2 - \frac{2(1 - k^2)}{1 - k^2 sn^2 u}\right)du\right]_{\xi_-}^{\xi_+}$$

$$B_r = \frac{\mu ni}{\pi}\sqrt{\frac{a}{r}}\left[\frac{2 - k^2}{2k}K(k) - \frac{E(k)}{k}\right]_{\xi_-}^{\xi_+} \tag{9}$$

E-900

where

$$k^2 = \frac{4ar}{\xi^2 + (a + r)^2} \tag{10}$$

In a similar manner, B_z (eq. (8)) can be reduced to standard elliptic integrals. First change the variable of integration to $t = \cos\theta$, and then use formulas 233.19 and 413.06 of reference 5. There follows successively

$$B_z = \frac{\mu ni}{4\pi\sqrt{2ar}}\int_{-1}^{+1}\left[\frac{\xi\left(\frac{a}{r} - t\right)dt}{\left(\frac{r^2 + a^2}{2ar} - t\right)\sqrt{(1 - t^2)\left(\frac{\xi^2 + r^2 + a^2}{2ar} - t\right)}}\right]_{\xi_-}^{\xi_+}$$

$$B_z = \frac{\mu ni}{2\pi(a + r)}\sqrt{\frac{a}{r}}\left[\xi k\int_0^K \frac{1 - \frac{2r}{a + r}sn^2 u}{1 - \frac{4ar}{(a + r)^2}sn^2 u}du\right]_{\xi_-}^{\xi_+}$$

$$B_z = \frac{\mu ni}{4}\left[\frac{\xi k}{\pi\sqrt{ar}}K(k) + \frac{(a - r)\xi}{|(a - r)\xi|}\lambda_o(\varphi,k)\right]_{\xi_-}^{\xi_+} \tag{11}$$

where

$$\varphi = \tan^{-1}\left|\frac{\xi}{a - r}\right| \tag{12}$$

As before, k is given by equation (10). The Heuman lambda function $\lambda_o(\varphi,k)$ is tabulated in references 5 and 6.

For many purposes, it is convenient simply to know the variation of the fields near the axis. As $r \to 0$, equations (9) and (11) reduce to the following well-known expressions:

$$B_r = \frac{\mu ni}{4}\left[\frac{a^2 r}{(\xi^2 + a^2)^{3/2}}\right]_{\xi_-}^{\xi_+} \tag{13}$$

$$B_z = \frac{\mu n i}{2}\left[\frac{\xi}{\sqrt{\xi^2 + a^2}}\right]_{\xi_-}^{\xi_+} \tag{14}$$

A convenient approximation for B_z, valid whenever $r \leqslant a$ and accurate to 1 percent in this range, is

$$B_z = \frac{\mu n i}{4}\left[\frac{\xi}{|\xi|}\left\{m(1 + 2k')\frac{2\varphi}{\pi} + \left[\frac{m^2(1 - m)}{4} + 2k'\right]\sin\varphi\right\}\right]_{\xi_-}^{\xi_+} \tag{15}$$

where $m = (1 - k')/(1 + k')$, $k' = \sqrt{1 - k^2}$. Equation (15) reduces exactly to equation (14) at the axis.

E-900

CALCULATIONS

Equations (9) and (11) are readily written in dimensionless form with the distances given in units of the solenoid radius. Then equations (9) to (14) still hold but with 1, r/a, $\xi_\pm/a$ replacing a, r, $\xi_\pm$ throughout.

Plots of the dimensionless axial and radial fields, $+4B_z/\mu n i$, $-4B_r/\mu n i$, are given in figures 1 and 2, respectively. Calculations were made for the ratio of coil length to radius in the range from 1 to 25. Note that in figures 1 and 2 the radial distance is given in terms of the coil radius (r/a) and, the axial distance is given in terms of the coil half-length ($2z/L$).

Discussion

The figures clearly show that increasing solenoid length decreases the radial variation of the axial field. This result is expected since an infinitely long solenoid has a uniform field throughout. For short solenoid lengths (fig. 1(a)), the axial field increases rapidly from the center to the wall for positions near the center of the solenoid. In fact, at the center the curve approaches very closely that for a simple loop.

It should be noted that the radial field is always infinite at $2z/L = 1.0$ and $r/a = 1$. This point corresponds to the edge of the current sheet and would be expected to produce such a result.

In general, uniform fields with total variations of 1 percent can be achieved over as much as 60 percent of the internal volume of the solenoid if the length is 25 radii or greater.

The calculations presented herein are limited to solenoids with infinitely thin walls but the results can readily be used to find approximate solutions for various shaped solenoids of finite thickness with almost any current distribution. Since superposition principles apply, it is only necessary to approximate any odd-shaped solenoid by a number of thin-walled solenoids and add the fields resulting from each. The accuracy of the answer is, of course, dependent on the number of separate solenoidal rings used to approximate the actual shape.

E-900

It is interesting to note that the results obtained herein for magnetic fields are closely related to the velocity fields produced by a lifting helicopter rotor (e.g., ref. 7). The physical model is the same but the detailed methods of solution are widely different.

Lewis Research Center
National Aeronautics and Space Administration
Cleveland, Ohio, May 23, 1960

REFERENCES

1. Bishop, Amasa S.: Project Sherwood - The U.S. Program in Controlled Fusion. Addison-Wesley Pub., 1958.

2. Scott, William T.: The Physics of Electricity and Magnetism. John Wiley & Sons, Inc., 1959.

3. Mapother, Dillon E., and Snyder, James N.: The Axial Variation of the Magnetic Field in Solenoids of Finite Thickness. Tech. Rep. 5, Univ. Ill., Nov. 16, 1954. (Contract DA-11-022-ORd-992.)

4. Foelsch, Kuno: Magnetfeld und Induktivitaet einer zylindrischen Spule. Archiv f. Elektrotech., Bd. XXX, Heft 3, Mar. 10, 1936, pp. 139-157.

5. Byrd, Paul F., and Friedman, Morris D.: Handbook of Elliptic Integrals for Engineers and Physicists. Springer-Verlag (Berlin), 1954.

6. Heuman, Carl: Tables of Complete Elliptic Integrals. Jour. Math. Phys., vol. 20, Apr. 1941, pp. 127-207.

7. Castles, Walter, Jr., and DeLeeuw, Jacob Henri: The Normal Component of the Induced Velocity in the Vicinity of a Lifting Rotor and Some Examples of Its Application. NACA Rep. 1184, 1954.

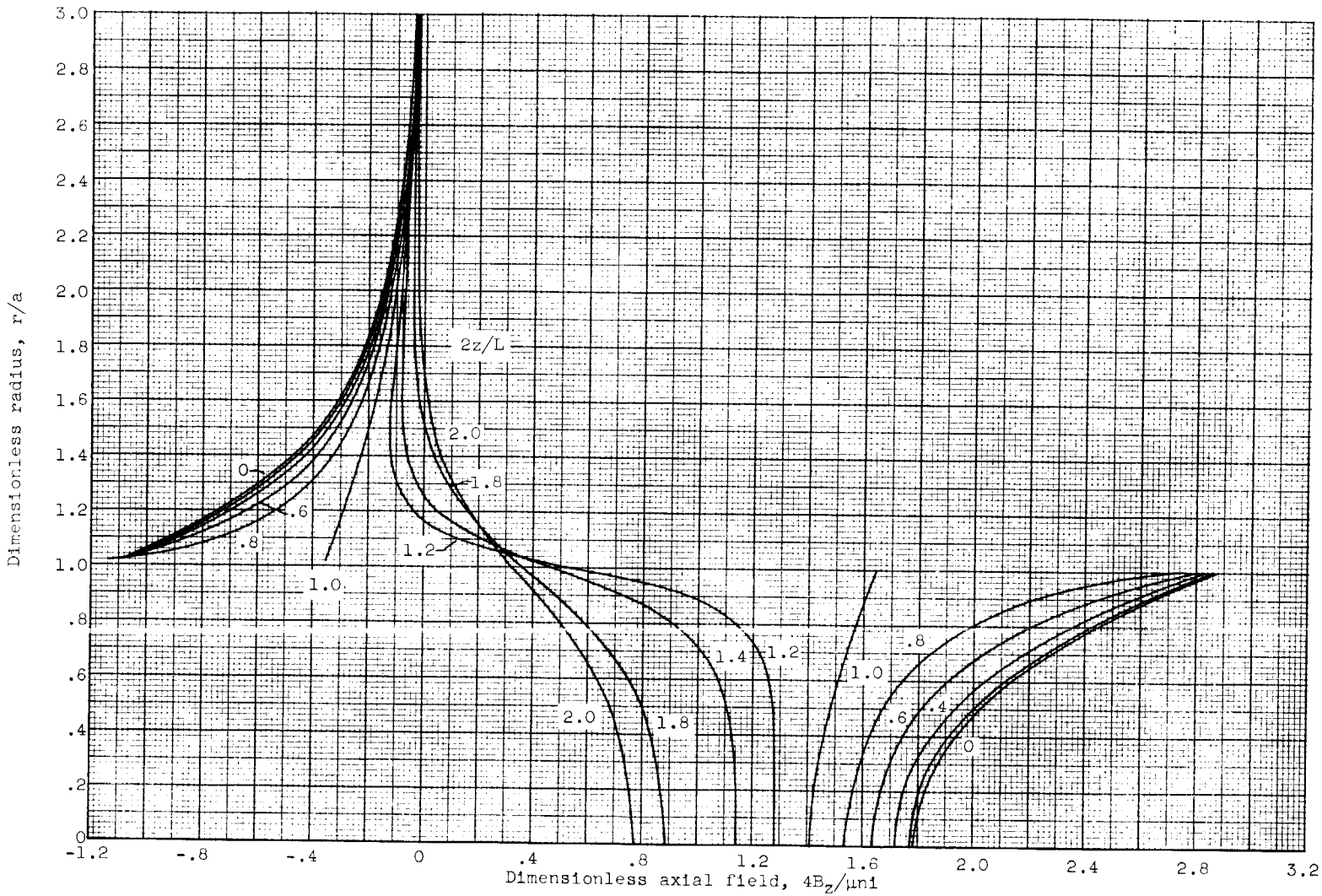

(a) L/a = 1.

Figure 1. - Dimensionless axial field of a finite solenoid.

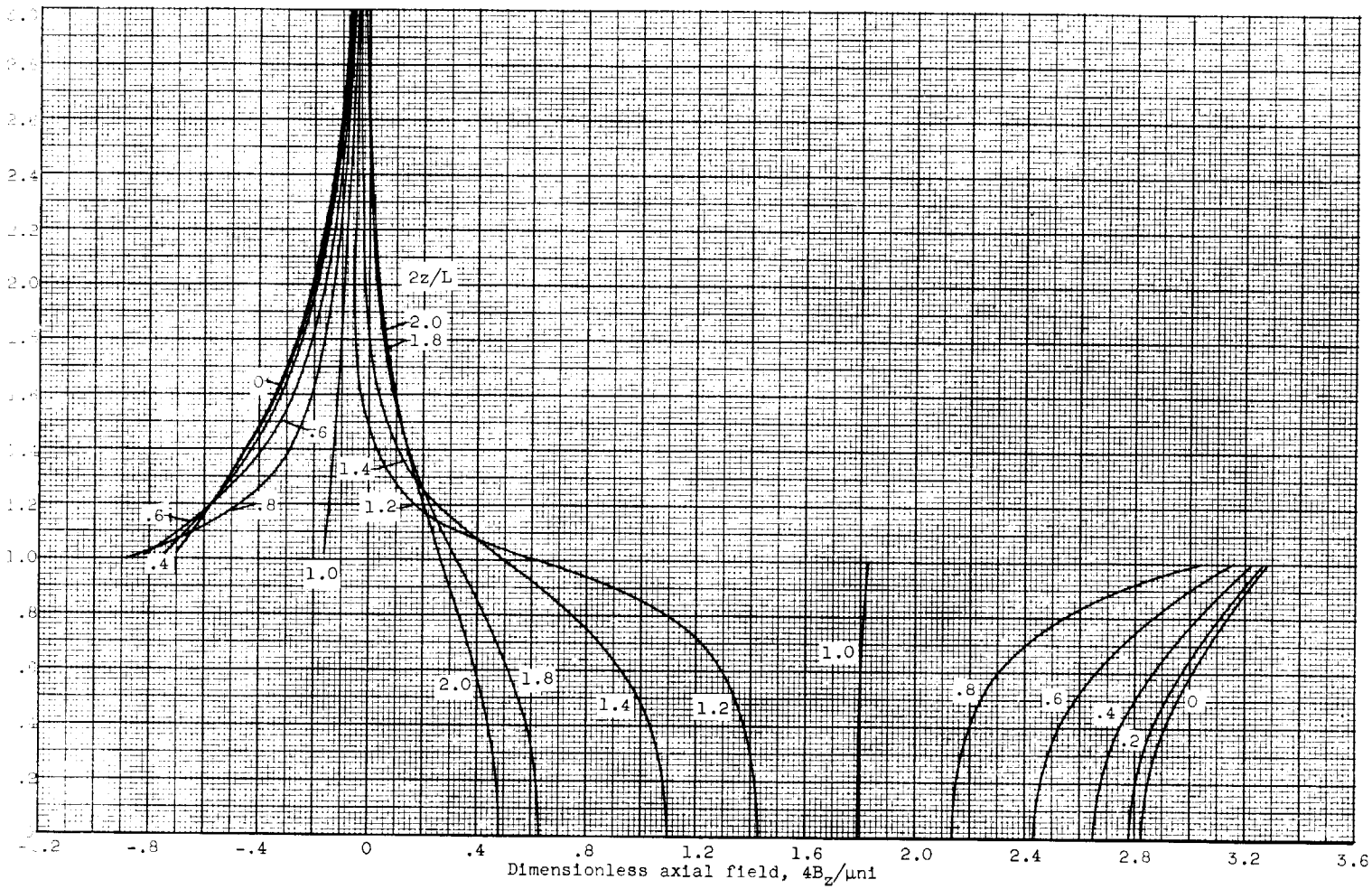

(b) L/a = 2.

Figure 1. - Continued. Dimensionless axial field of a finite solenoid.

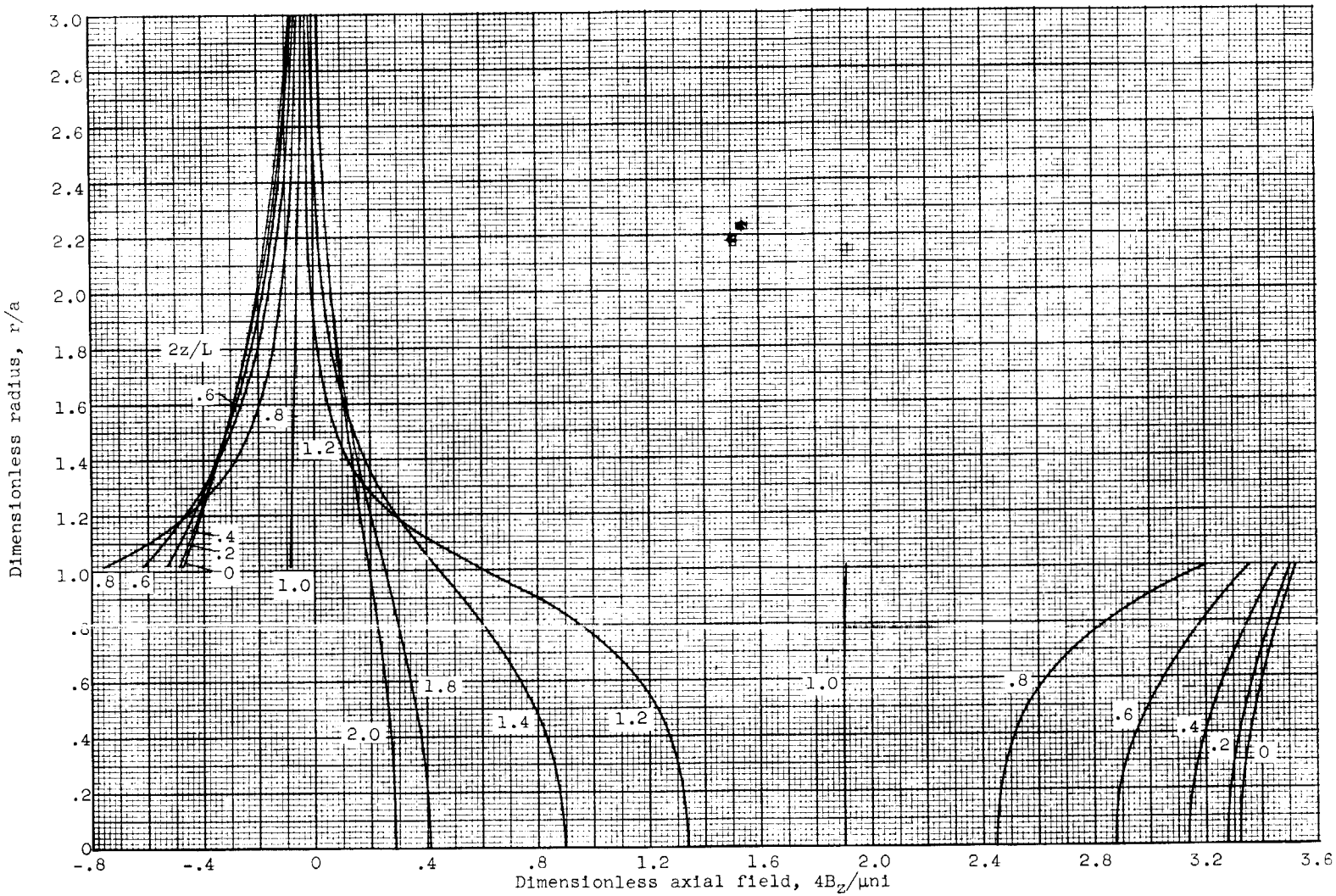

(c) L/a = 3.

Figure 1. - Continued. Dimensionless axial field of a finite solenoid.

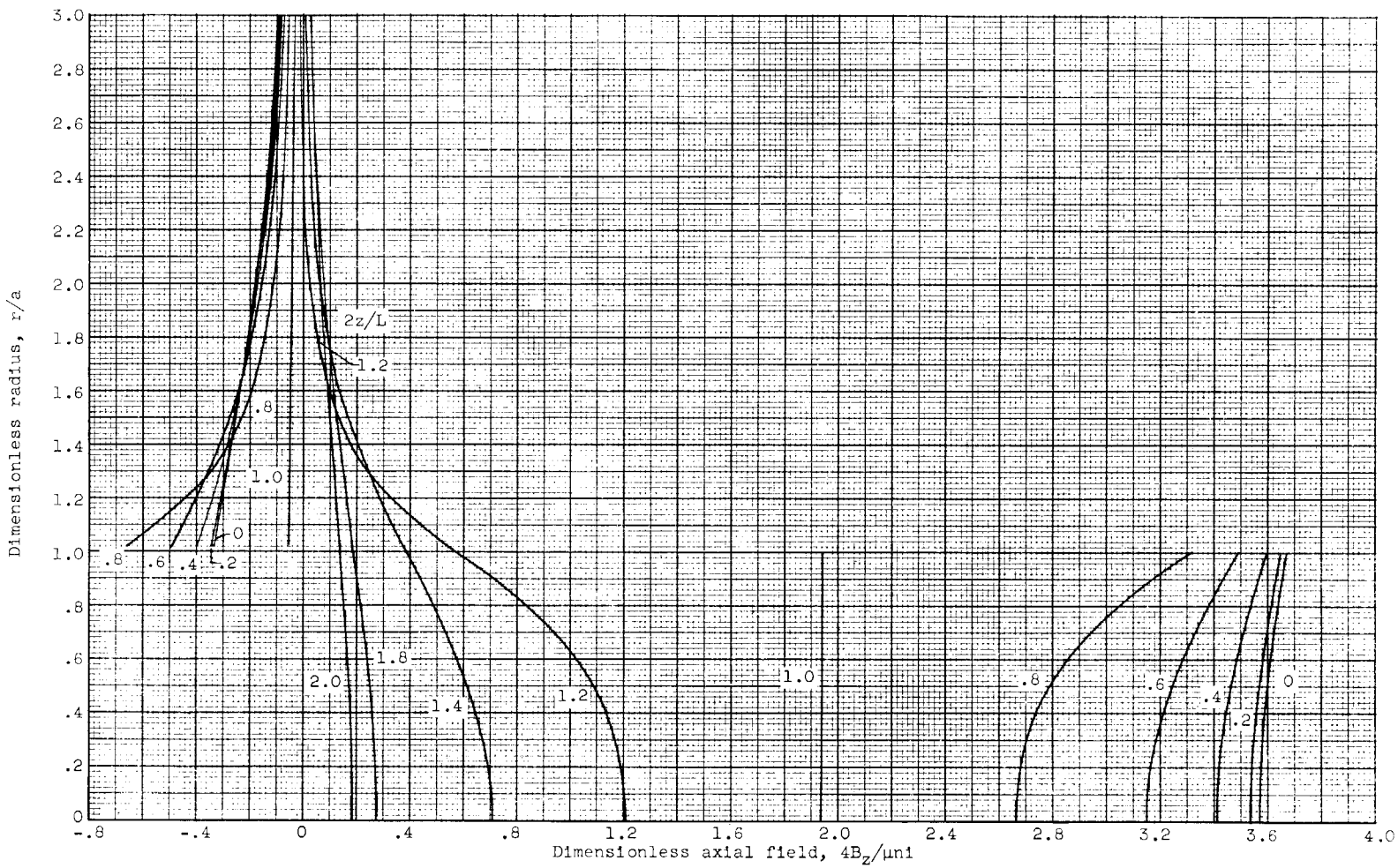

(d) L/a = 4.

Figure 1. - Continued. Dimensionless axial field of a finite solenoid.

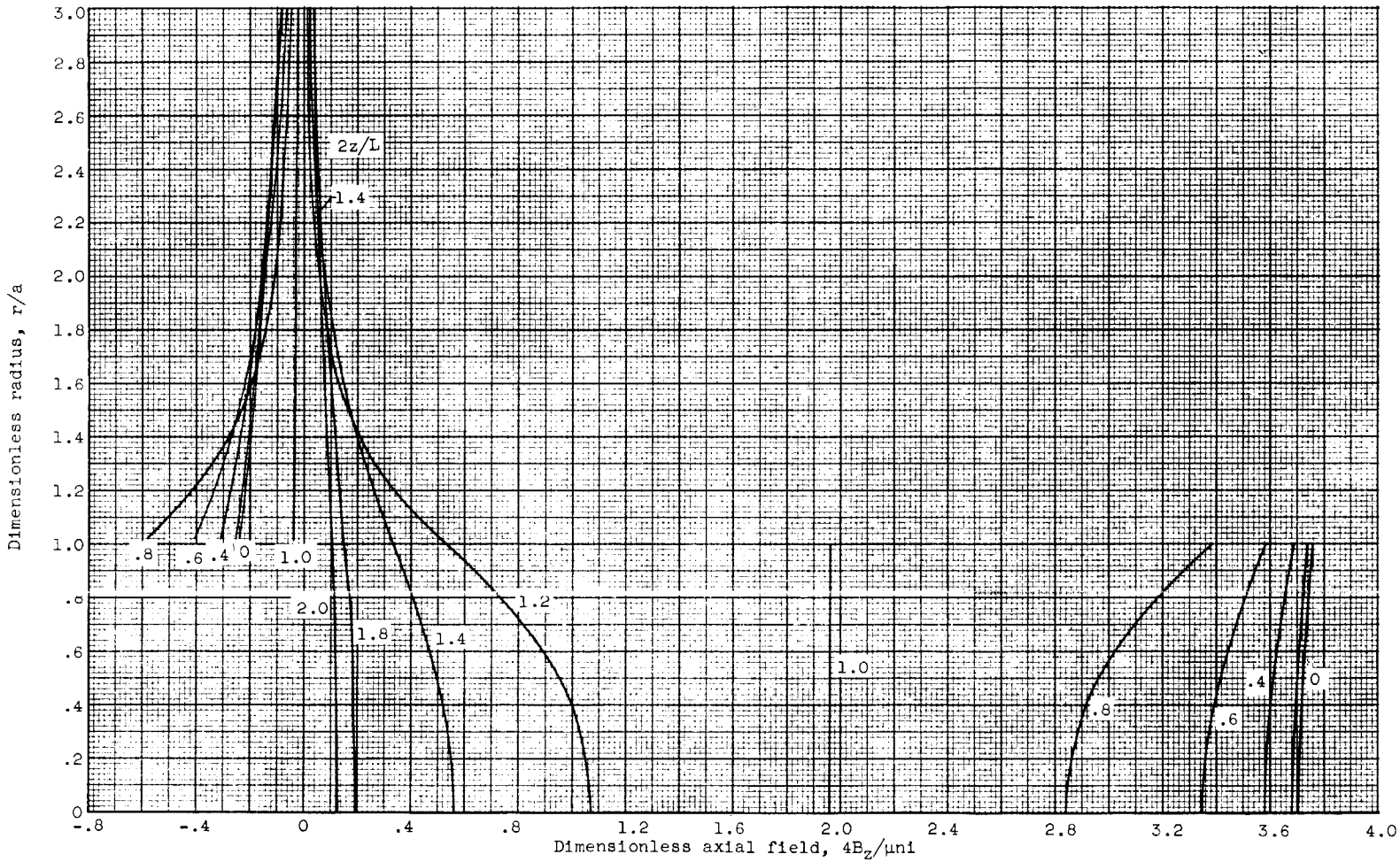

(e) L/a = 5.

Figure 1. - Continued. Dimensionless axial field of a finite solenoid.

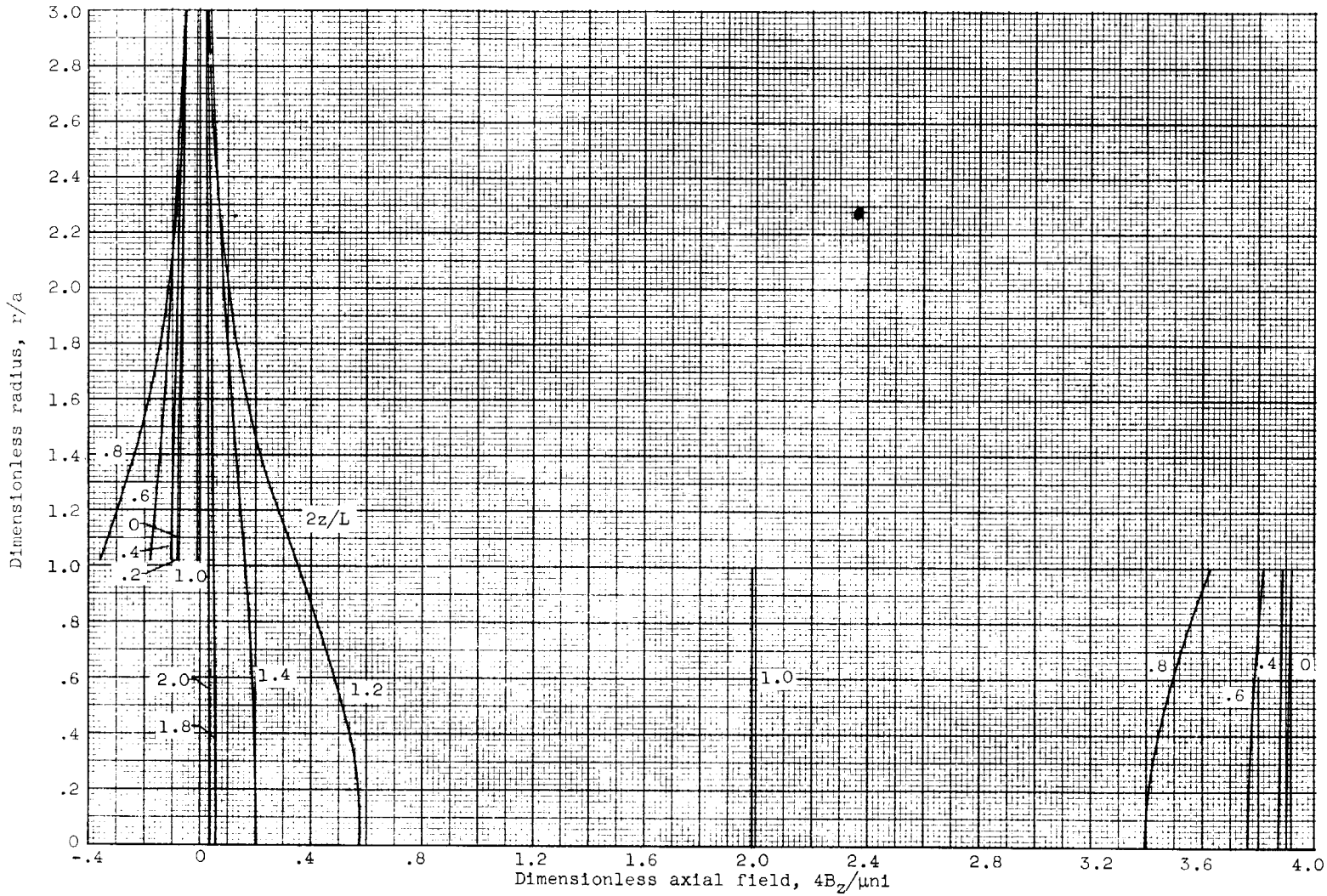

(f) L/a = 10.

Figure 1. - Continued. Dimensionless axial field of a finite solenoid.

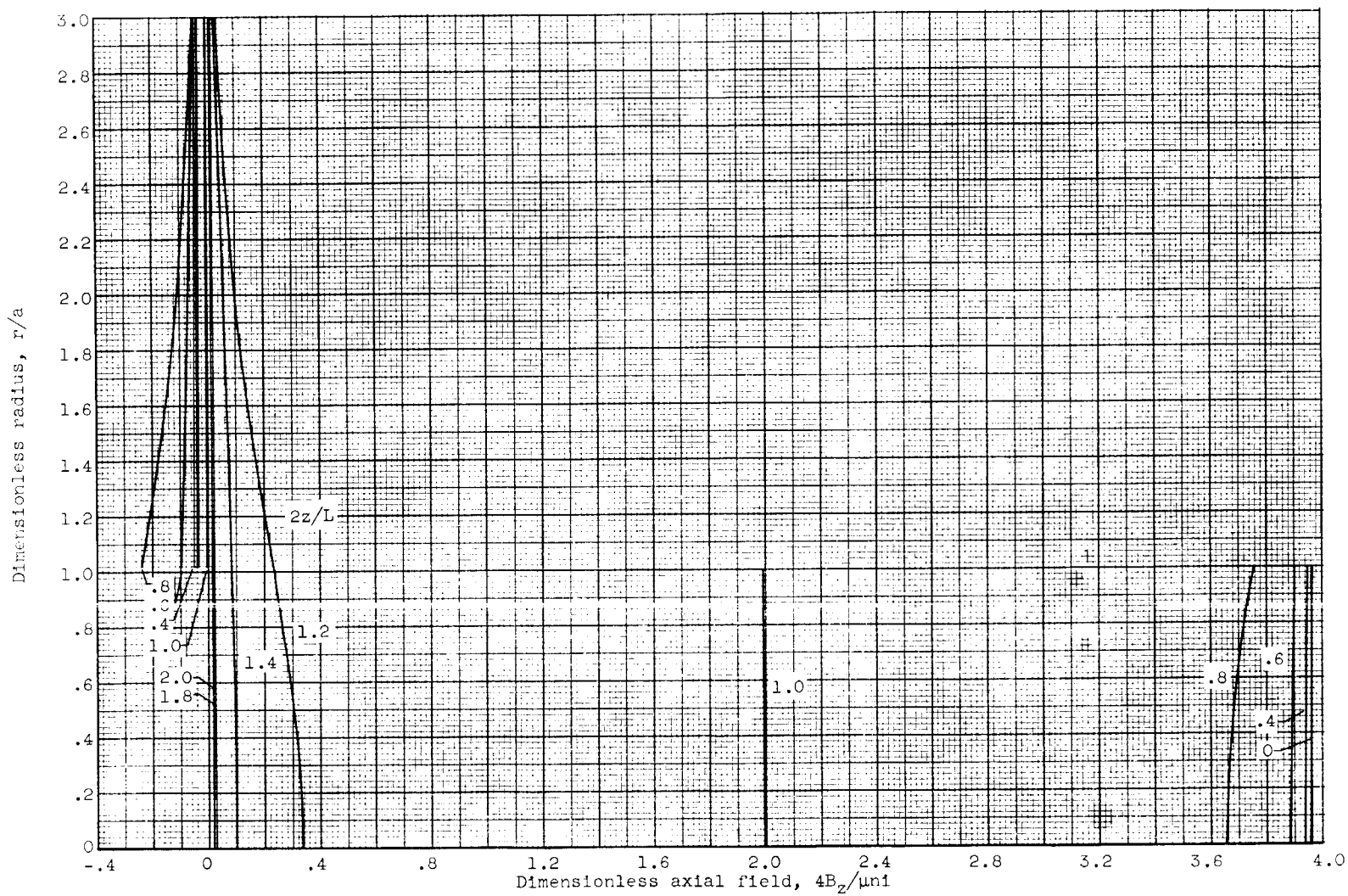

(g) L/a = 15.

Figure 1. - Continued. Dimensionless axial field of a finite solenoid.

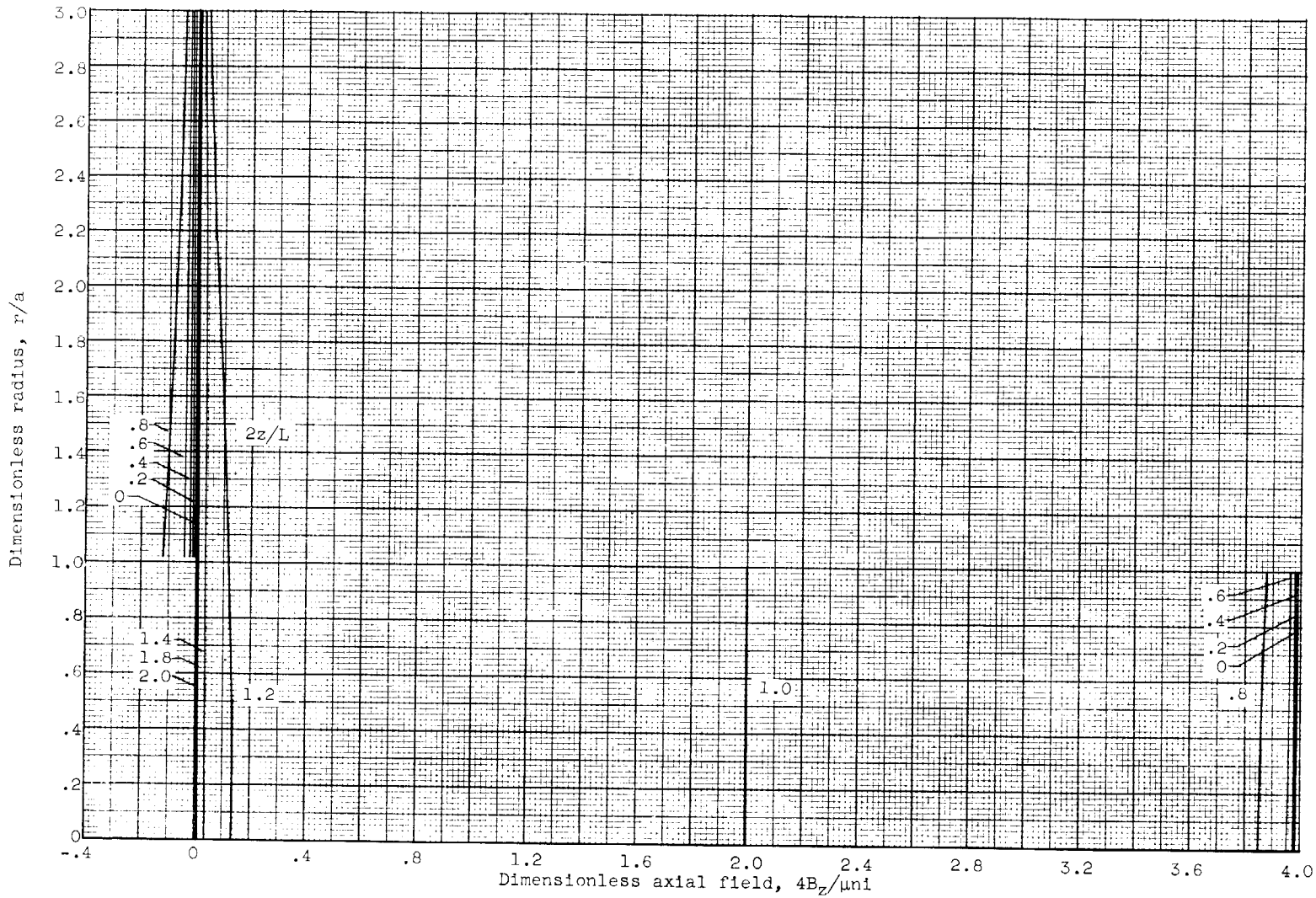

(h) L/a = 25.

Figure 1. - Concluded. Dimensionless axial field of a finite solenoid.

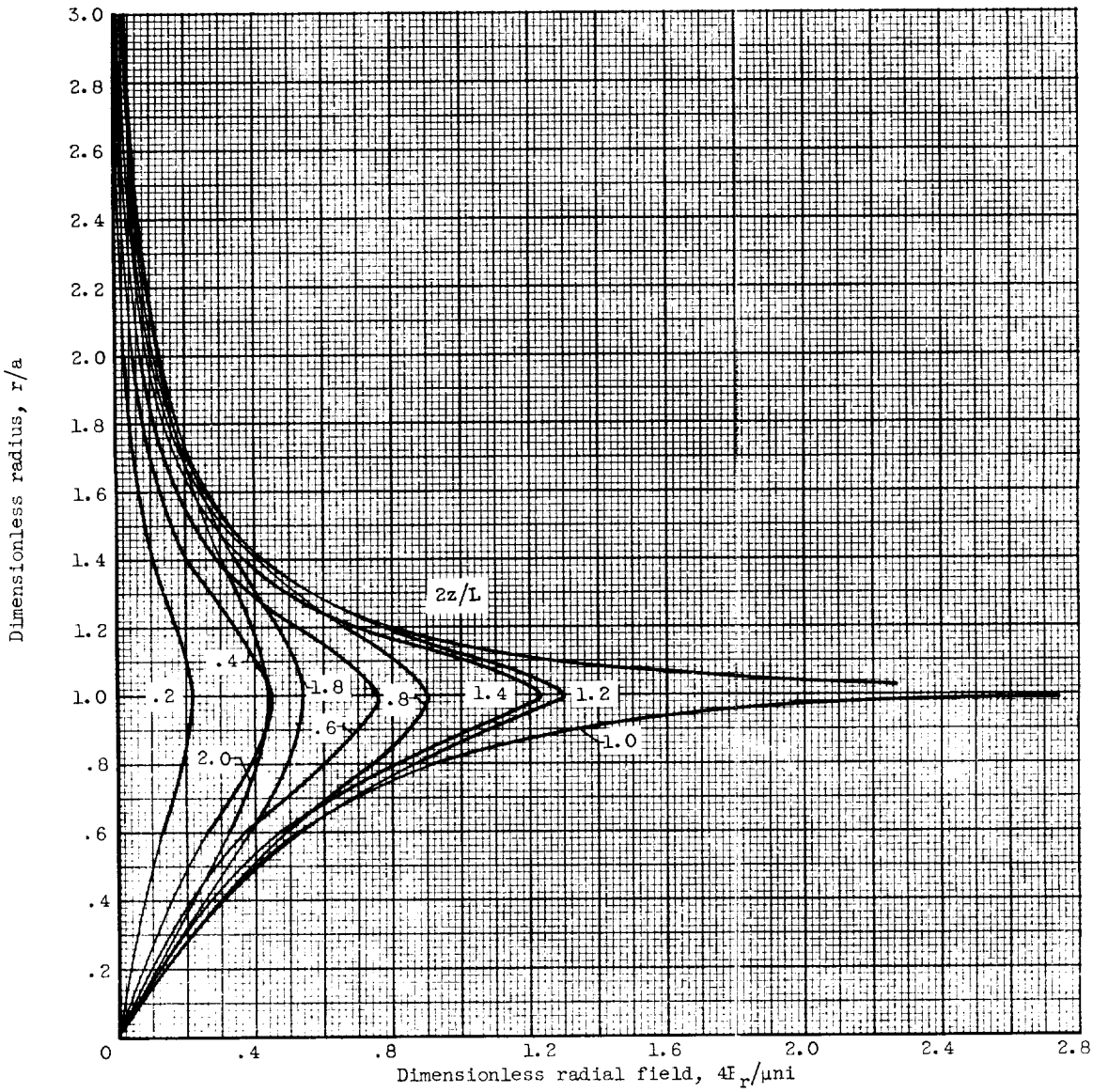

(a) L/a = 1.

Figure 2. - Dimensionless radial field of a finite solenoid.

E-900

E-900

CQ-3

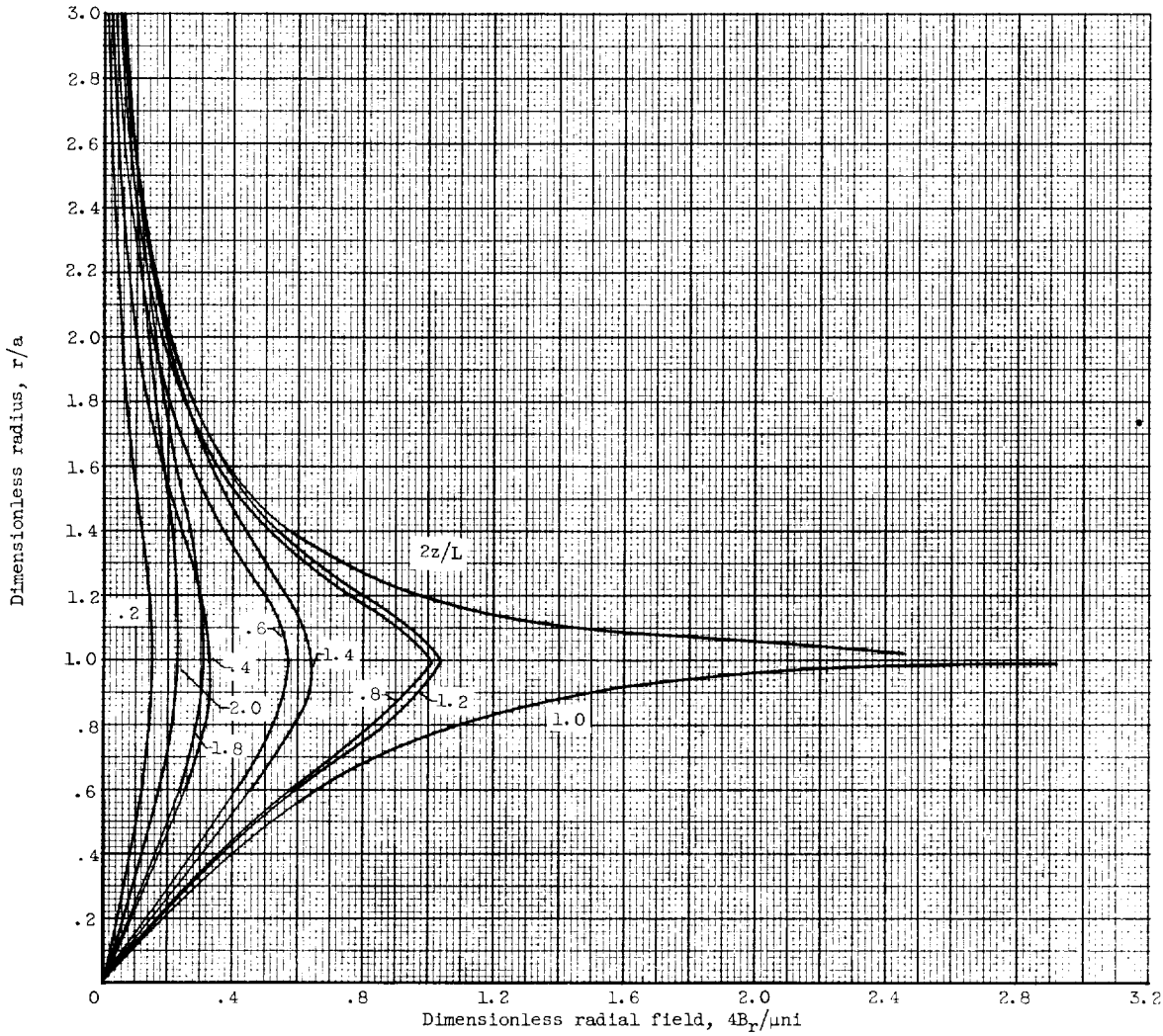

(b) L/a = 2.

Figure 2. - Continued. Dimensionless radial field of a finite solenoid.

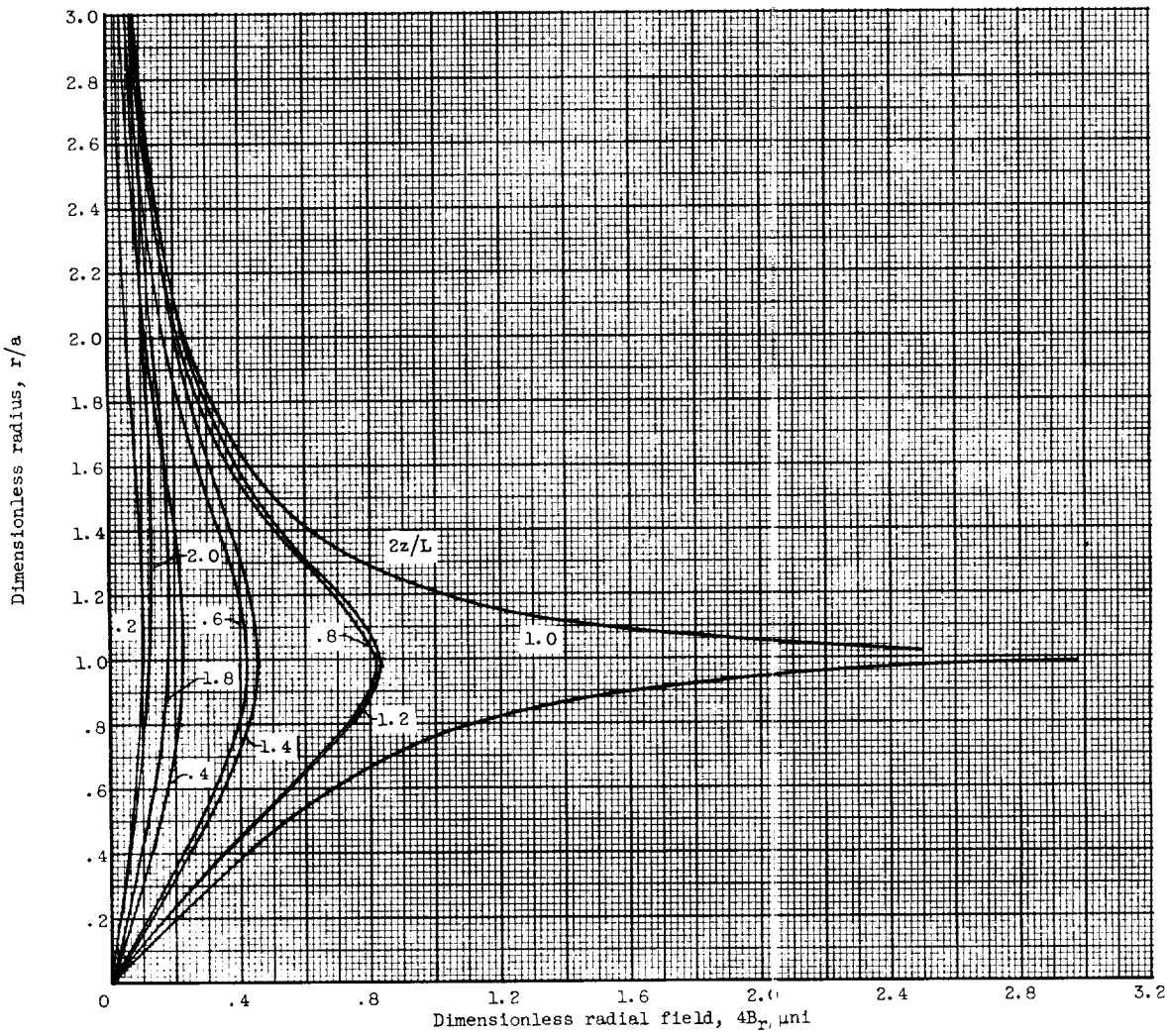

(c) L/a = 3.

Figure 2. - Continued. Dimensionless radial field of a finite solenoid.

E-900

E-900

CQ-3 back

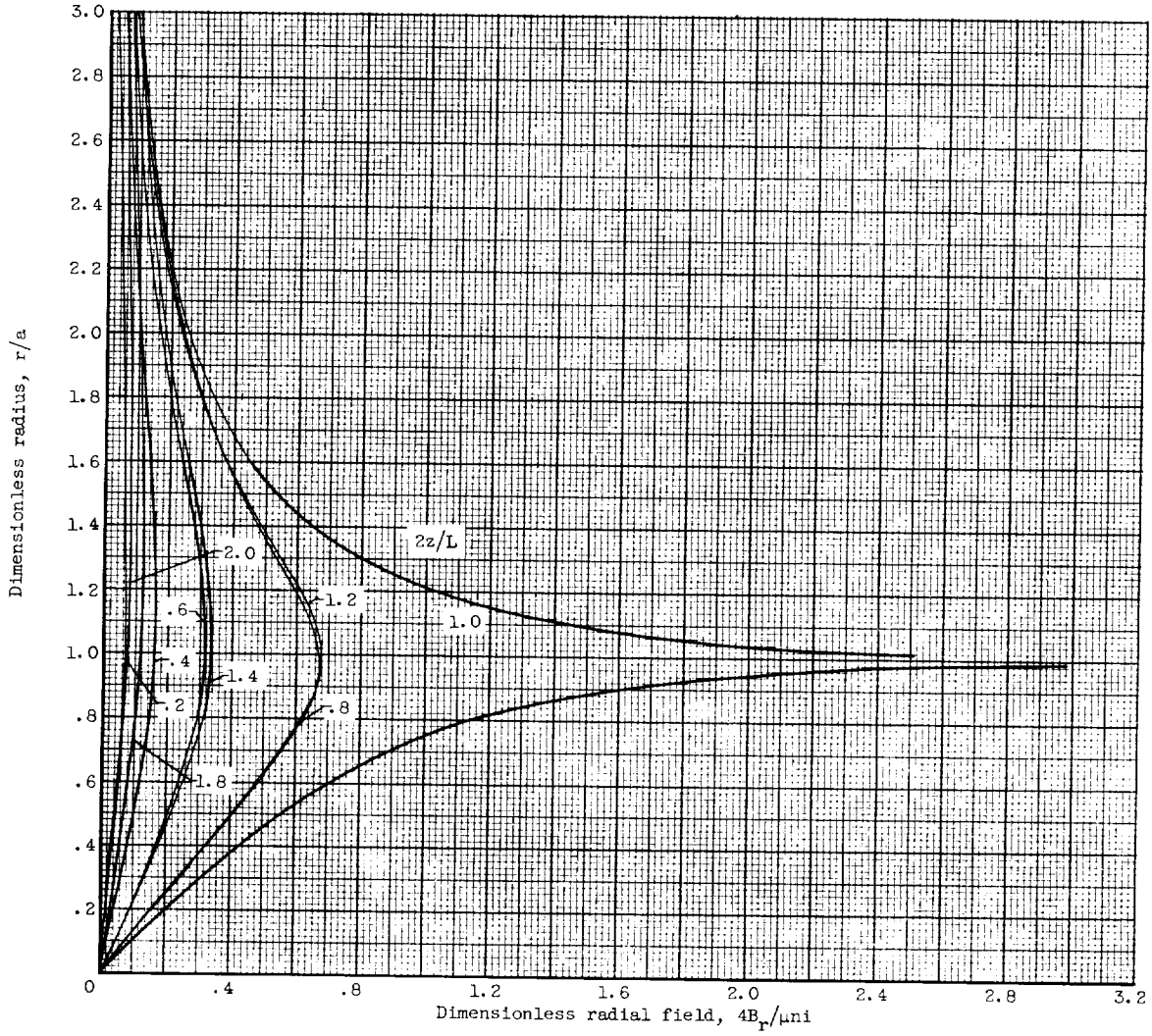

(d) L/a = 4.

Figure 2. - Continued. Dimensionless radial field of a finite solenoid.

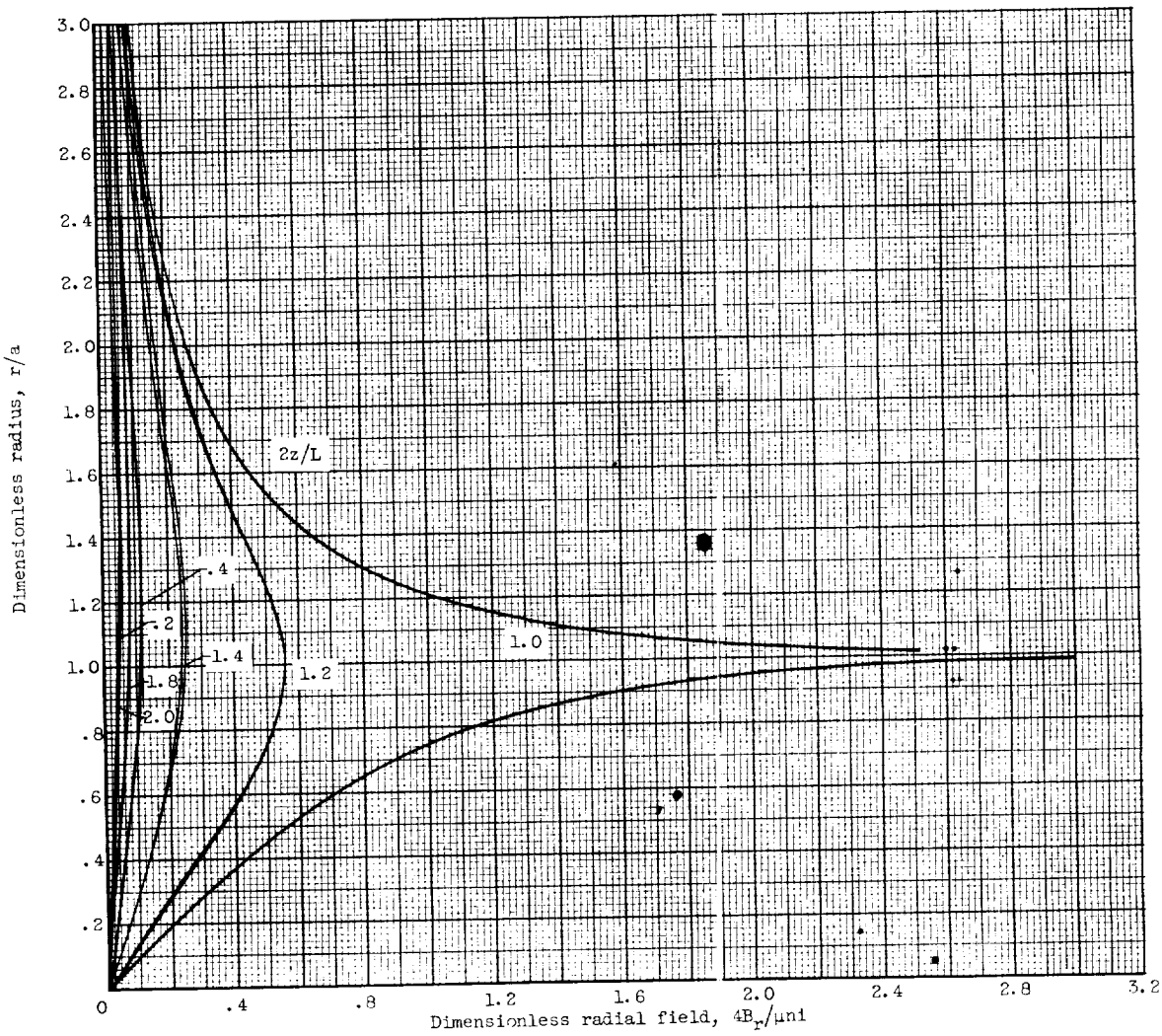

(e) L/a = 5.

Figure 2. - Continued. Dimensionless radial field of a finite solenoid.

E-900

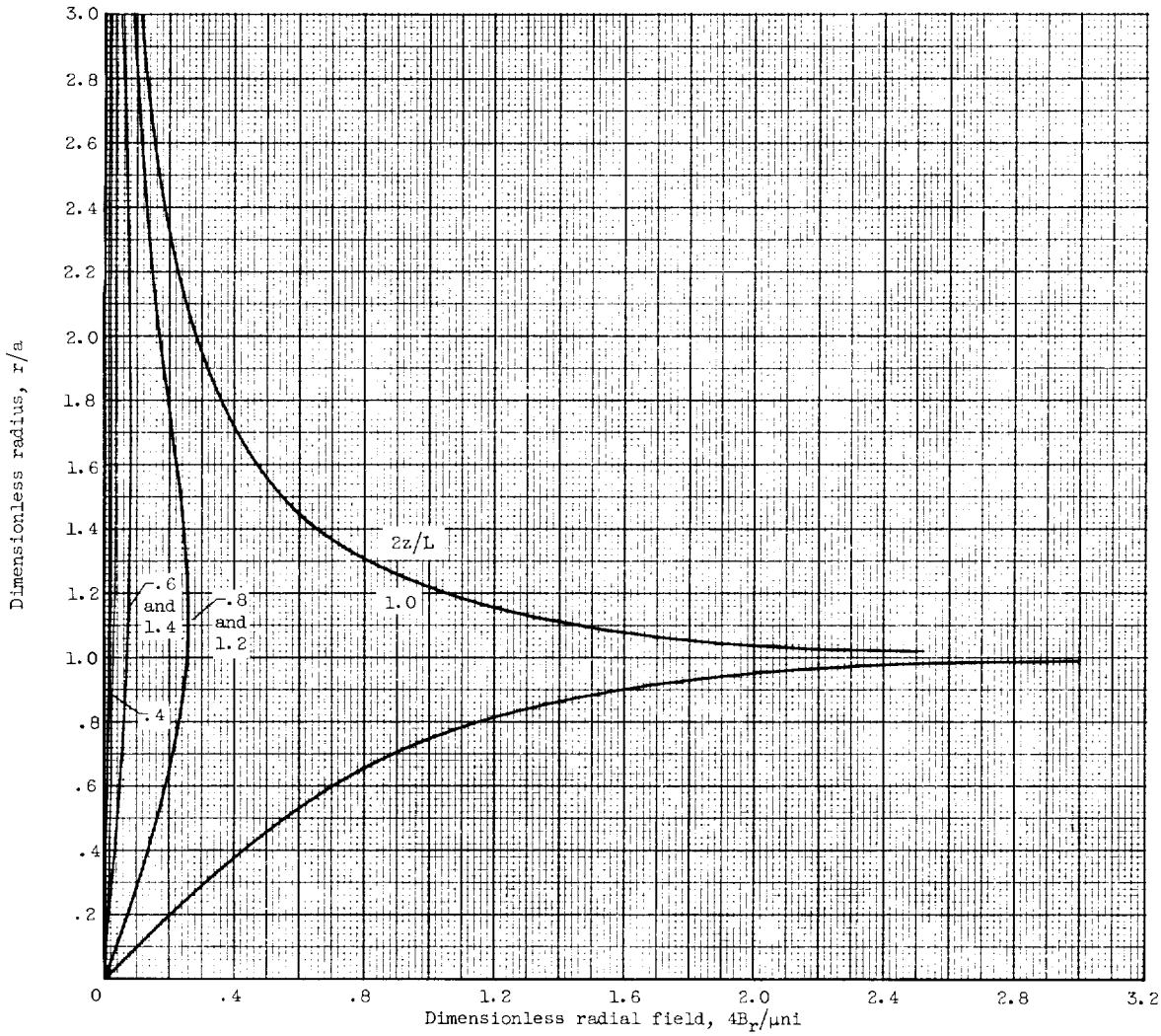

(f) L/a = 10.

Figure 2. - Continued. Dimensionless radial field of a finite solenoid.

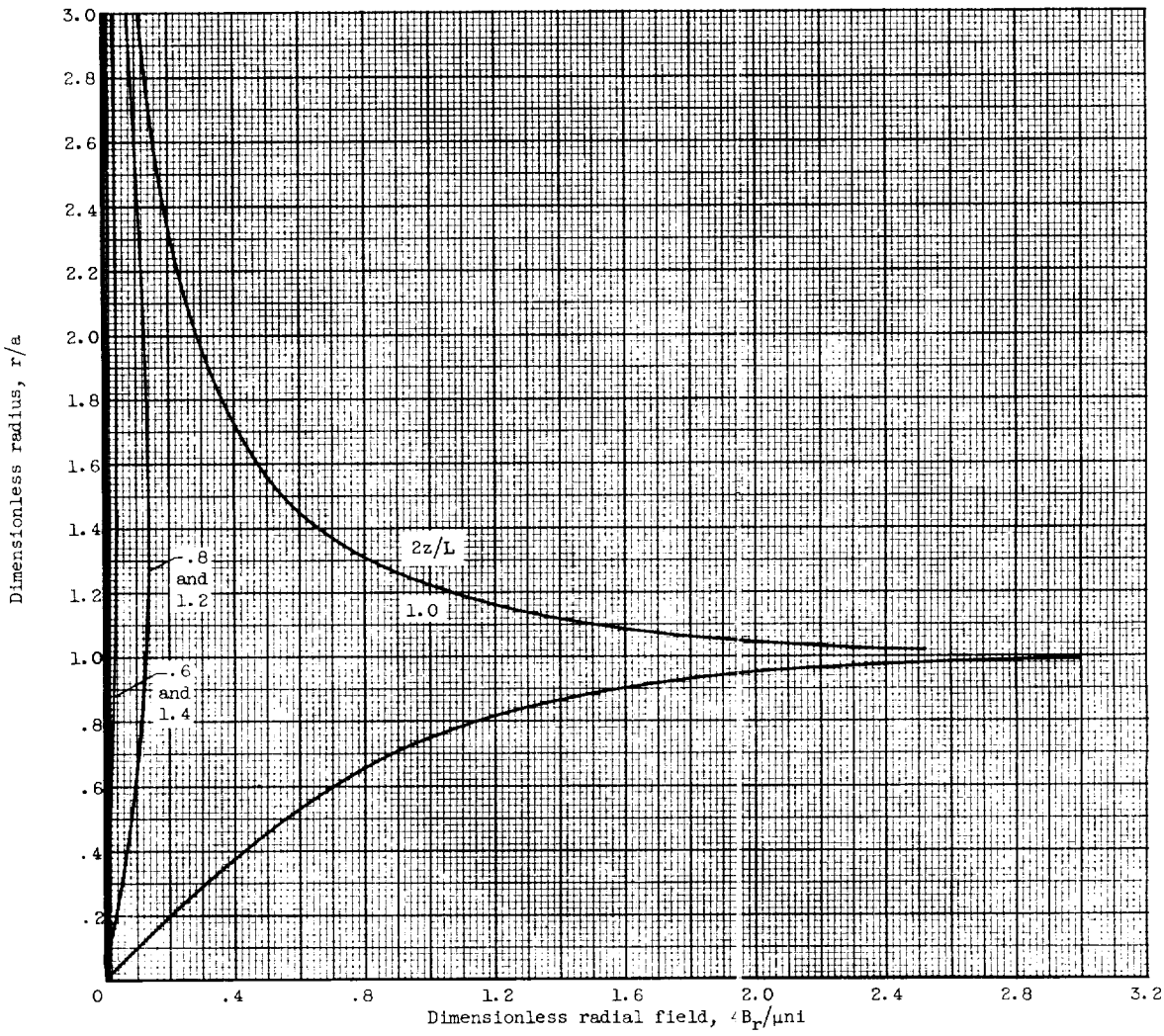

(g) L/a = 15.

Figure 2. - Continued. Dimensionless radial field of a finite solenoid.

E-900

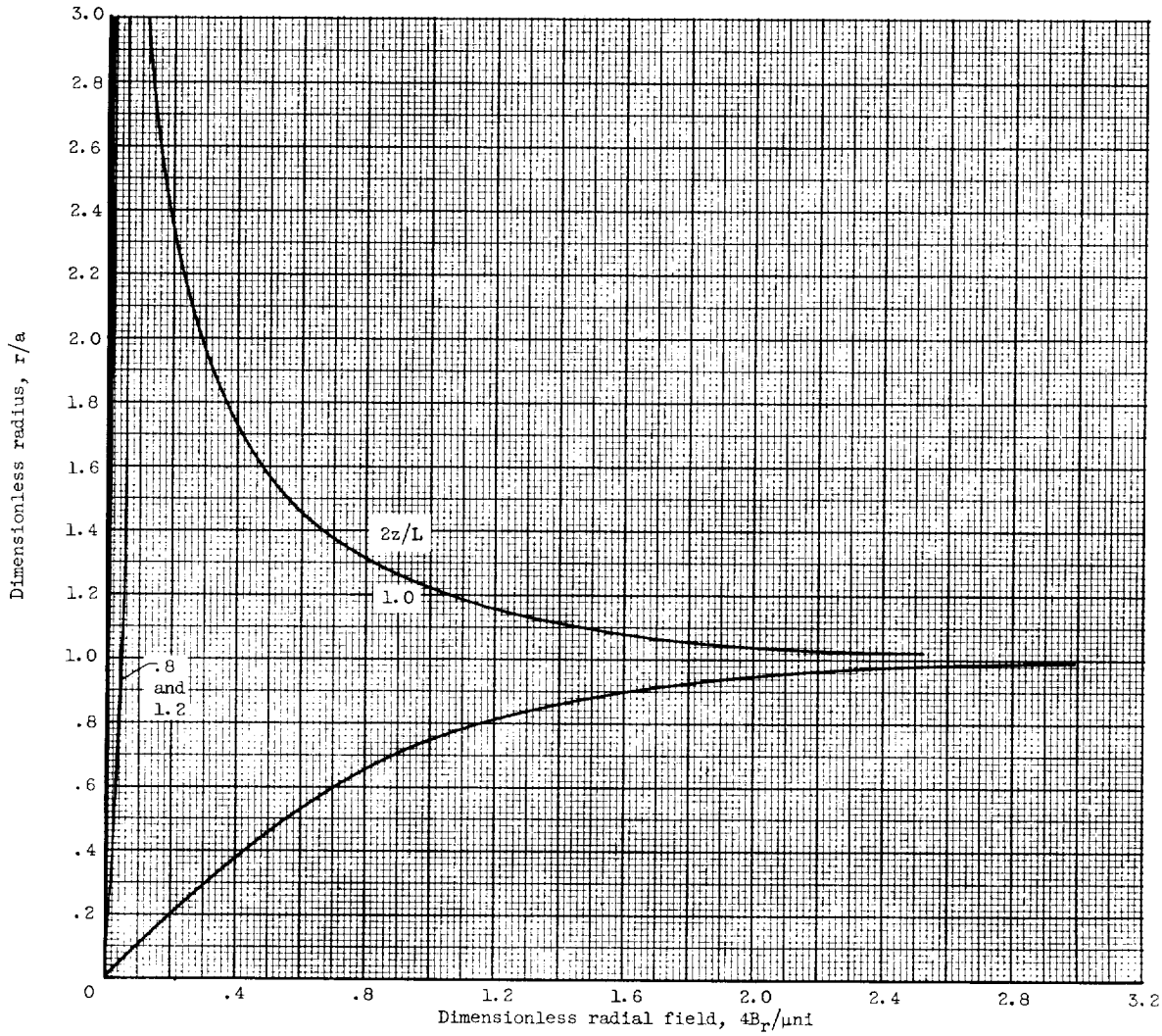

(h) L/a = 25.

Figure 2. - Concluded. Dimensionless radial field of a finite solenoid.

NASA - Langley Field, Va. E-999